Magmatic salt melt and vapor

Extreme fluids forming porphyry gold deposits in shallow subvolcanic settings

This is the Green Open Access version of: Koděra, P., Heinrich, C.A., Wälle, M. and Lexa, J., 2014. Magmatic salt melt and vapor: Extreme fluids forming porphyry gold deposits in shallow subvolcanic settings. *Geology*, vol. 42, pp. 495-498.
https://doi.org/10.1130/G35270.1

Magmatic salt melt and vapor: Extreme fluids forming porphyry gold deposits in shallow subvolcanic settings

Peter Koděra[1], Christoph A. Heinrich[2], Markus Wälle[2], and Jaroslav Lexa[3]
[1]Department of Geology of Mineral Deposits, Faculty of Natural Sciences, Comenius University, Mlynská dolina, 842 15 Bratislava, Slovakia
[2]Department of Earth Sciences, ETH Zürich, 8092 Zürich, Switzerland
[3]Geological Institute, Slovak Academy of Sciences, Dúbravská cesta 9, 840 05 Bratislava, Slovakia

Abstract

The recently discovered Biely Vrch deposit in the Western Carpathian magmatic arc is the most extreme example of a porphyry gold deposit, being practically free of copper, molybdenum or any other sulfide minerals. Microanalytical data on fluid inclusions in quartz veinlets, including a characteristic type of banded veinlets, show that this deposit formed from nearly anhydrous Fe-K-Na-Cl salt melts containing ~10 ppm Au, coexisting with hydrous vapor of very low density. This exceptional fluid evolution required an Fe-rich dioritic source magma that was emplaced at shallow subvolcanic depth (<3.5 km), directly exsolving a hypersaline liquid and magmatic vapor at high temperature (~850 °C). During ascent to the level of the porphyry intrusion (0.5 – 1 km), fluid expansion at high temperature but low pressure led to halite precipitation and further water loss to the vapor, generating an increasingly Fe-K-rich salt melt that transported high concentrations of Au but negligible Cu into the fractured porphyry stock. The low sulfur fugacity resulting from fluid expansion suppressed precipitation of sulfide, explaining the gold-only enrichment in this globally-recurring but rather rare type of gold ore.

1. Introduction

Porphyry gold deposits represent a distinct type of economic gold ore devoid of economically mineable copper (< 0.15 wt%), in contrast to more common porphyry Cu ± Au ± Mo deposits (Sillitoe, 2010). They are characterized by a bulk-mineable network of commonly banded quartz-magnetite veinlets hosted by small subvolcanic intrusions of rather mafic (typically dioritic) calc-alkaline magma (Vila and Sillitoe, 1991; Sillitoe, 2000). Porphyry gold deposits are known from only a few global ore provinces, including the classical Maricunga belt in N Chile (Muntean and Einaudi, 2001), the Middle Cauca belt in Columbia (Garzon, 2011), the South Apuseni Mountains in Romania (Ruff et al., 2012) and the Javorie belt in Slovakia (Hanes et al., 2010). The reasons for their restricted occurrence remains unclear. Some authors have linked them to exceptional tectono-magmatic conditions favoring partial melting of a gold enriched source in the mantle (Richards, 2009; Loucks, 2012). Others emphasise selective metal precipitation by an extreme degree of fluid phase separation along a specific pressure – temperature path in shallow subvolcanic settings, involving a deep supercritical magmatic fluid that successively separates into vapor + hypersaline aqueous liquid and eventually reaches the vapor + halite field (Muntean and Einaudi, 2000, 2001). In this paper we report the discovery of nearly anhydrous gold-rich salt melts of exceptionally $FeCl_2$ and KCl rich composition. Based on microanalytical and published experimental data we propose a link between

the two alternative interpretations, explaining why specific source magmas as well as an extreme fluid evolution path may be required to generate these new but potentially important gold resources.

2. Beily Vrch porphyry gold system

Porphyry gold deposits occur in the central zone of the Javorie andesite stratovolcano in the Central Slovakia Volcanic Field (Western Carpathians; Fig. 1). The stratovolcano evolved in several stages during the Middle Miocene (Konečný et al., 1998), with Au-mineralization hosted by stocks of biotite-hornblende diorite porphyry (Hanes et al., 2010). The recently discovered Biely Vrch deposit (34 t Au @ 0.8 g/t Au) is a typical example with an exceptionally low Cu/Au ratio even among porphyry Au deposits (0.018 wt% Cu / ppm Au; Hanes et al., 2010). Paleovolcanic reconstruction indicates that the tops of the porphyry intrusions have reached a depth of ~500 m below the paleosurface, similar to the Marte deposit in the Maricunga Belt (Vila et al., 1991). Argillic alteration largely overprinted earlier K-silicate alteration at shallow and Ca-Na silicate alteration at deeper levels (>400 m below surface). Compared to the more common Cu-Au porphyry deposits, the vertical extent of these high-temperature alteration zones is very short, consistent with a very shallow emplacement of the parental intrusion.

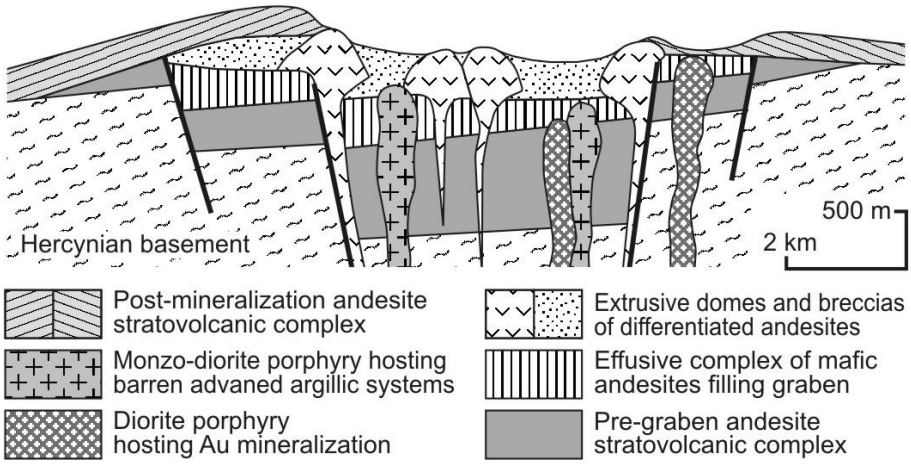

Figure 1. Simplified section of the Javorie stratovolcano hosting porphyry gold systems in a central volcanotectonic graben zone (adapted from Konečný et al., 1998).

Several generations of veinlets are present, forming a dense stockwork. They include early biotite-magnetite and granular quartz veinlets with irregular vein walls, resembling A-veinlets of Gustafson and Hunt (1975). Somewhat later banded quartz veinlets are a distinct characteristic of Biely Vrch and many other porphyry Au deposits (Muntean and Einaudi, 2000; Ruff et al., 2012), containing abundant micron-sized magnetite grains and vapor inclusions aligned in wall-parallel bands (Fig. 2A). The bands are often botryoidal and continuous through several quartz grains, suggesting that the quartz recrystallized from amorphous silica that was precipitated due to rapid fluid decompression (Herrington and Wilkinson, 1993; Muntean and Einaudi, 2000). Locally, rare xenoliths of vein quartz occur entrapped in porphyry, indicating multi-stage veining and intrusion activity in the magmatic-hydrothermal system. Gold mineralization is coincident with the most densely veined parts of quartz stockwork. High fineness gold grains occur next to quartz veinlets in altered wall rock, together with clay minerals and chlorite replacing K-feldspar and magnetite. Rare sulfide veinlets (mostly pyrite, chalcopyrite) cut or infill the quartz stockwork veins and are also related to this argillic alteration (Koděra et al., 2010).

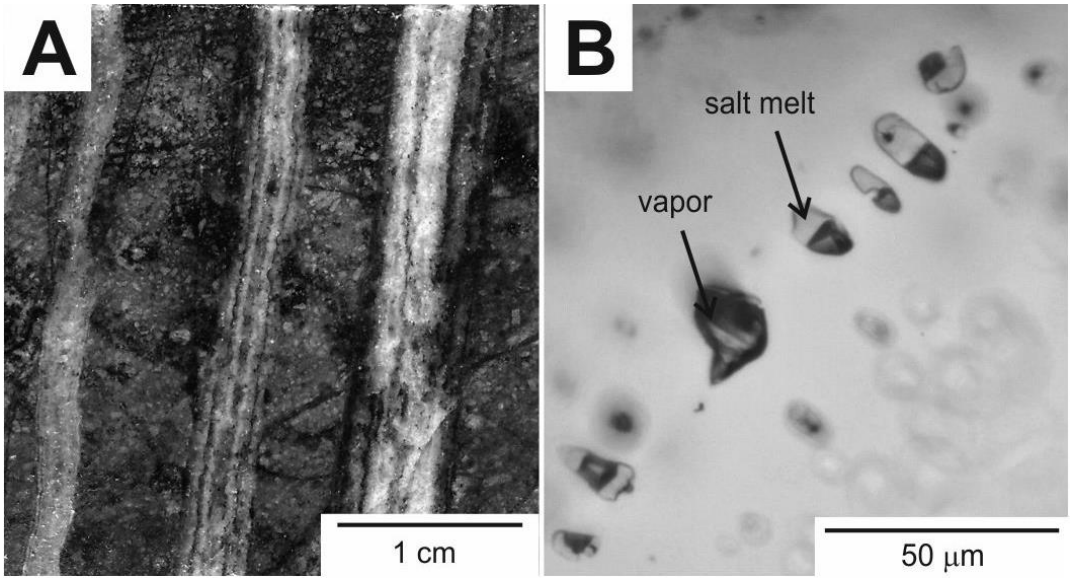

Figure 2. Images from the Biely Vrch porphyry gold deposit: **A**. Quartz stockwork including banded veinlets. **B**. Trail of coexisting salt melt and vapor inclusions hosted in granular vein quartz.

3. Fluid composition and temperature

Four types of fluid inclusions have been recognized at Biely Vrch: rare brine inclusions (type B) restricted to the deepest parts of the porphyry and xenoliths brought up from below the ore zone; ubiquitous vapor inclusions (type V) and unusual but widespread salt melt inclusions (type S) associated with porphyry gold mineralization, locally coexisting on single healed microfractures (Fig. 2B); and minor secondary aqueous inclusions of variable salinity, associated with argillic alteration (type L).

Similar to porphyry gold deposits in the Maricunga Belt, apparently empty vapor inclusions (type V) are the dominant type of inclusions in all stockwork veins and especially the banded veinlets. They show no phase changes during cooling or heating, indicating very low bulk density.

Assemblages of unusual inclusions containing consistent phase proportions of several salt crystals are associated with coeval vapor inclusions at Biely Vrch (Fig. 2B). More than half of the volume of these salt inclusions is occupied by a green anisotropic crystal. Smaller halite or sylvite crystals are not always discernible but typically occupy 20 volume percent and are accompanied by one or two smaller salt grains with higher refractive index. The remaining space (up to 30% by volume) is filled with a distorted vapor bubble. There is no aqueous liquid visible at room temperature, even in sharp corners of some of the inclusions. Based on Raman spectroscopy (see digital Repository[1]), all solid phases except one of the smaller grains are water-free, indicating that these inclusions represent an essentially anhydrous salt melt. Such salt melt inclusions are common in granular vein quartz, which is bright in cathodoluminiscence imaging (CL) and formed between near-magmatic temperatures (up to ~725°C) and at least ~590 °C, based on Ti-in-quartz thermometry (Koděra et al., 2013), but similar inclusions also occur in darker-luminescent quartz varieties including the banded veinlets, formed at temperatures down to 380 °C (Ti detection limit; Koděra et al., 2013).

Heating of the salt melt inclusions led to rapid melting of all major solids between 321 and 361 °C (mostly 321–333 °C), sometimes followed by dissolution of a discernible halite crystal above ~400 °C. After melting of solids, inclusions contained a well-visible round bubble that did not reach liquid-

[1] GSA Data Repository item 2014177, is available online at www.geosociety.org/pubs/ft2014.htm, or on request from editing@geosociety.org or Documents Secretary, GSA, P.O. Box 9140, Boulder, CO 80301, USA.

vapor homogenization (T_h) up to 850 °C. Although some of these inclusions were probably trapped at near-magmatic temperature, the highest T_h values may result from modification of density due to the □- to □-quartz transition, and/or heterogeneous entrapment of some vapor with the salt melt.

LA-ICPMS microanalyses[1] were applied to inclusions from variable depth. All salt melt inclusions and most vapor inclusions suitable for quantitative analysis were hosted by granular vein quartz (mostly primary, but some on secondary trails), whereas the banded quartz is too crowded for controlled ablation of individual inclusions. S-type inclusion assemblages contain the major elements Fe-K-Na-Cl in near-constant proportions. Charge balance between major cations and Cl ranges from 0.5 to 1.6 (median 1.1) indicating ~50 wt% $FeCl_2$, ~30 wt% KCl and ~20 wt% NaCl (Figs. 3A). A compositional trend in a Na-K-Fe ternary plot roughly points toward $NaCl_{75}KCl_{25}$, on the halite – sylvite join, consistent with precipitation of K-bearing halite from fluids that cooled from high temperature (cf. Cloke and Kesler, 1979). V-type inclusions show similar element proportions as S-type inclusions and probably represent signals from minor salt melt trapped as preferentially surface-wetting phase with the vapor. Some individual inclusions from banded quartz show extreme Fe contents, probably due to concurrent ablation of submicroscopic magnetite grains.

The gold concentration of salt melt and vapor inclusions, expressed as a weight fraction of total NaCl+KCl+$FeCl_2$ (see Repository Table 1) varies between 0.3 and 43 ppm, whereas the corresponding fraction for Cu is only ~100 times higher. The Au/Cu ratio in these inclusions is similar to or even higher than the bulk metal ratio in the Biely Vrch deposit (Figs. 3B), and more than 10x higher than the bulk metal ratio of the Maricunga porphyry gold ores (Muntean and Einaudi, 2001). Au/Cu ratios in the Biely Vrch inclusions are more than two orders of magnitude higher than in brines and vapors forming typical porphyry Cu-Au deposits like Bajo de la Alumbrera or Grasberg, where the metal ratios in the fluids were also found to approximately match that of the bulk orebodies (Ulrich et al., 1999). As a significant exception, two samples representing quartz vein xenoliths entrapped in porphyry from Biely Vrch have relatively higher Cu contents both in S- and V-type inclusions, more similar to those forming porphyry-Cu-Au deposits (Fig. 3B), indicating an earlier episode of porphyry fluids and mineralization.

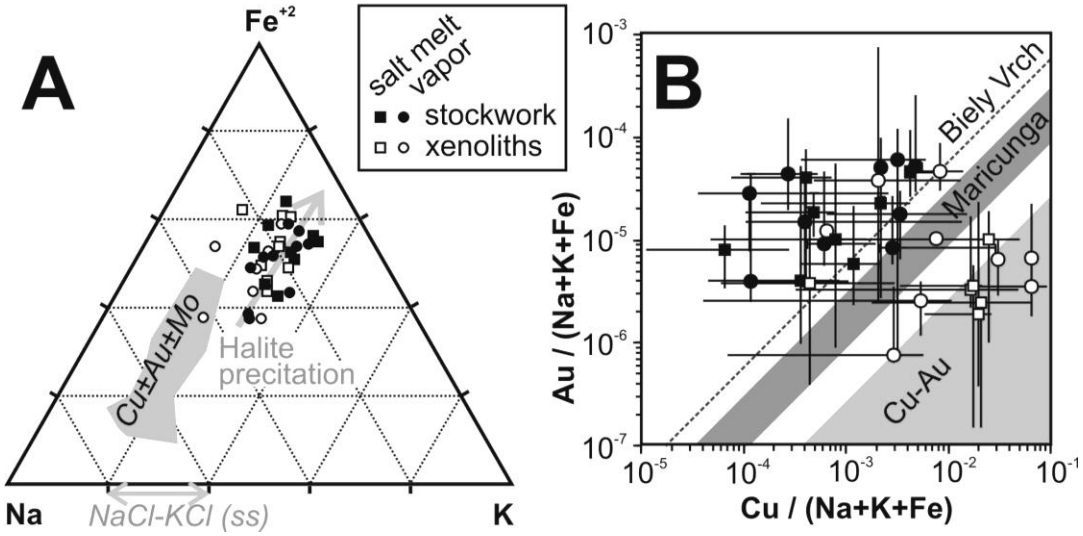

Figure 3. LA-ICPMS microanalyses of fluid inclusions from the Biely Vrch deposit (mean values of inclusion assemblages): **A**. Molar variation of major cations with interpretation of major trends and composition of fluids in Cu ± Au ± Mo porphyry deposits for comparison (data compiled from literature1). **B**. Copper versus gold concentrations. Diagonal bands show average Cu/Au ratios of ores at Biely Vrch, Maricunga porphyry Au deposits, and of porphyry Cu-Au deposits worldwide.

4. From magmatic fluid to gold-mineralizing salt melt + vapor

The fluid evolution near the magmatic fluid source below Biely Vrch can be schematically interpreted with reference to the binary phase diagram of the system NaCl-H_2O (Fig. 4A; Driesner and Heinrich 2007), but our observations also require consideration of experimental data on complex salt melts at lower temperatures and at the low water pressures prevailing in the ore-depositional environment (Fig. 4B; Robelin et al., 2004). Based on the water-saturated solidus of silicic magmas (e.g., Holtz et al., 2001), the Biely Vrch diorite porphyry was emplaced at ~850 °C. Considering the stability of amphibole and biotite in silicic magmas (e.g., Holtz et al., 2005; Rutherford and Hill, 1993), reaction coronas of biotite and amphibole phenocrysts indicate that a parental magma chamber of that temperature was located at shallow depth (P < 1–1.5 kbar). Vapor exsolution at ~1 kbar and ~850 °C will directly form a highly saline brine (~70 wt% salt) coexisting with vapor (Driesner and Heinrich, 2008). If the two fluid phases are expelled together towards shallower levels (~1 km; Fournier, 1999; Weis et al., 2012), decompression and adiabatic cooling to ~725°C (max. temperature of quartz veinlets) would lead to a low-salinity water vapor with <~0.02 wt % salt, coexisting with a highly saline brine or hydrous salt melt (equivalent to ~90 wt% NaCl). In the NaCl-H_2O model system, such fluids will reach halite saturation at high temperature (>600°C on vapor+liquid+halite surface in Fig. 4A). Subsequent cooling would occur in the halite + vapor field without aqueous liquid, but in a more complex K-Fe-rich system a molten salt phase remains stable to lower temperatures, as shown by NaCl-KCl-$FeCl_2$ experiments (Robelin et al., 2004; Fig. 4B). NaCl is the highest-melting salt in the anhydrous system, so that saturation with halite (NaCl-KCl solid solution) occurs first after further cooling. The remaining salt melt becomes progressively enriched in $FeCl_2$ and KCl, until the molten salts eutectically solidify at 330–309 °C. This evolution path explains the observed trends of changing K/Na and Fe/Na ratios of analyzed inclusions (Fig. 3A) and their microthermometric behavior. Early cooling of the deep brine to salt melt and vapor (discussed above) resulted in the precipitation of granular quartz veinlets and magnetite, hosted by potassic alteration (Fig. 4A). On cooling below 400 °C, the volumetrically dominant vapor expanded further by transition from lithostatic to hydrostatic pressure, leading to further dehydration of the Fe-K-rich salt melt. The banded quartz veins probably formed at this transition, as a result of supersaturation with respect to amorphous silica and co-precipitation of magnetite with minor gold.

Our microanalytical data indicate that transport and precipitation of gold at Biely Vrch was effected, at least in part, by the Fe-K-Na-Cl-rich salt melt. The density of the coexisting vapor was probably too low to enable significant metal solubility (Williams-Jones and Heinrich, 2005; Hurtig and Williams-Jones, 2014), consistent with a very low sulfur fugacity that prevented the formation of gold bisulfide complexes as well as the precipitation of any sulfide minerals (Muntean and Einaudi, 2000). Gold solubility in salt melt is not known experimentally, so we cannot evaluate gold speciation and precipitation reactions. However, our results suggest that the proposed mineralization process is fundamentally different from gold transport and precipitation in other gold-rich porphyry to epithermal systems (green fluid path in Fig. 4A), where gold is deposited by expanding dense vapor (e.g., Bingham Canyon porphyry Cu-Au-Mo; Landtwing et al., 2010) or from a low-salinity aqueous liquid derived by cooling and contraction of magmatic vapor at higher pressure (epithermal deposits; Hedenquist et al., 1998; Heinrich et al., 2004).

The major-element trend of brine to salt melt evolution (Fig. 3A) shows that the high Fe/Na and K/Na ratios in Au porphyry fluids are driven by halite precipitation on ascent, but a pre-enrichment of Fe and K has probably occurred already at the stage of fluid exsolution from a relatively mafic magma. Our compilation of published LA-ICPMS data[1] shows that fluids in most Au-bearing porphyry deposits are enriched in Fe and K compared to fluids in other types of porphyry deposits that are associated with more silicic magmas, and that the Fe-K enrichment of fluids correlates with their Au/Cu ratio. Experimental work of Zajacz et al. (2012a) showed that for andesitic melts in upper crustal magma chambers, K and Fe partition more strongly into a Cl-bearing fluid phase (relative to

Na) compared to felsic systems, thus generating initial fluid compositions that can evolve toward a K-Fe-rich salt melt during subsequent cooling and decompression. Mafic and alkali-rich magmas of moderately high oxidation level (around ΔNNO = +0.5) also have a higher volatile/melt partition coefficient for Au, relative to Cu and compared to more felsic melts, thus maximizing gold extraction into magmatic-hydrothermal fluids (Zajacz et al., 2012b; Botcharnikov et al., 2010).

These data indicate that the subsolidus evolution of magmatic fluids toward Fe- and Au-rich salt melts is favored by relatively mafic and alkalic source magmas. Magmatic source constraints can explain the provinciality of the global distribution of porphyry Au deposits, but they also seem to be a prerequisite for the unusual fluid evolution path toward Au-mineralizing salt melts. Mafic medium to high-K andesite magmas of the W Carpathians are thought to result from extension-related partial melting of previously metasomatized and oxidized lithospheric mantle (e.g., Harangi et al., 2007), and similar post-subduction settings (Richards, 2009) have been inferred for the Middle Cauca belt in Colombia (hosting the world-class porphyry gold deposit of La Colosa; Garzon, 2011) and the South Apuseni Mountains of Romania (Harris et al., 2013).

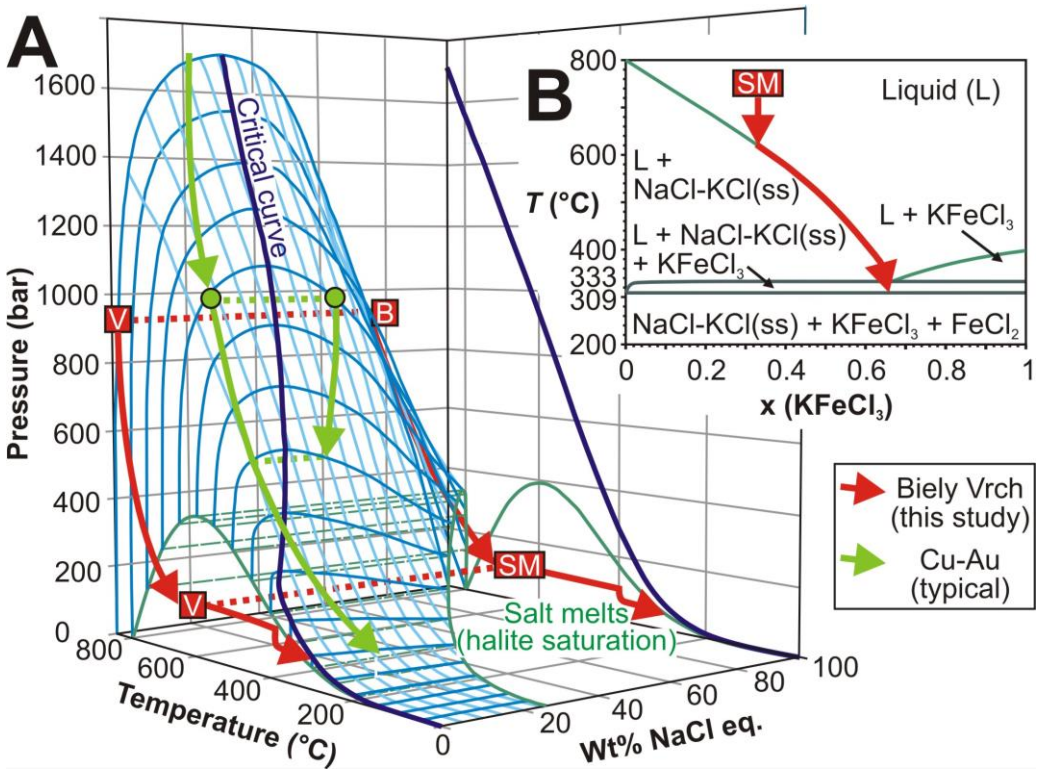

Figure 4. A. P–T–X_{NaCl} phase diagram (modified from Driesner and Heinrich, 2007), illustrating fluid pathway for magmatic–hydrothermal fluids at Biely Vrch (red arrows), which exsolved from magma in the two-phase vapor + brine field (V, B) and then cooled to a nearly anhydrous salt melt (SM) at low pressure; for comparison, deeper porphyry Cu ± Au fluids are denser and evolve to variably phase-separated aqueous solutions (green arrows). **B.** Salt melt evolution during cooling within the NaCl-KCl-$FeCl_2$ molten salt system (after Robelin et al., 2004).

5. Conclusions

Porphyry copper – gold deposits are formed from dense magmatic vapor coexisting with minor hypersaline liquid, which on cooling and expansion form concentrated ore shells by precipitation of gold with Cu-Fe-sulfides at ~400 °C and a characteristic depth of 1–3 km below the Earths surface (Sillitoe, 2010; Weis et al., 2012). Based on the observations at Biely Vrch, the comparatively rare prophyry gold deposits require the combination of three geological factors: (a) an Fe-rich high-K calc-

alkaline source magma from a mantle source that may have been enriched in Au by preceding subduction metasomatism and was re-melted in an extensional setting; (b) shallow subvolcanic emplacement of hot hydrous magma enabling direct exsolution of vapor and a K-Fe-enriched brine; and (c) rapid expansion and cooling of this two-phase fluid in a fumarolic environment, leading to the formation of an anhydrous K-Fe-rich salt melt transporting tens of ppm of gold and precipitating the precious metal with silica and magnetite but without sulfides. If this interpretation applies to other porphyry gold deposits, simple petrographic observation of entirely salt-filled inclusions with a distorted vacuole may help recognizing this new but possibly more widespread type of gold resource.

Acknowledgements

Support by the Slovak Research and Development Agency (contract No. 0537-10) and EMED Mining is acknowledged. Jarmila Luptáková is acknowledged for Raman spectroscopy analyses. We are grateful to Robert Bodnar, Jeremy Richards and other colleagues for clarifying comments on this paper.

References cited

Botcharnikov, R.E., Linnen, R.L., Wilke, M., Holtz, F., Jugo, P.J., and Berndt, J., 2010, High gold concentrations in sulphide-bearing magma under oxidizing conditions: Nature Geoscience, v. 4, p. 112–115, doi:10.1038/ngeo1042.

Cloke, P.L., and Kesler, S.E., 1979, The halite trend in hydrothermal solutions: Economic Geology and the Bulletin of the Society of Economic Geologists, v. 74, p. 1823–1831, doi:10.2113/gsecongeo.74.8.1823.

Driesner, T., and Heinrich, C.A., 2007, The system H_2O-NaCl. Part I: Correlation formulae for phase relations in temperature-pressure-composition space from 0 to 1000 °C, 0 to 5000 bar, and 0 to 1 XNaCl: Geochimica et Cosmochimica Acta, v. 71, p. 4880–4901, doi:10.1016/j.gca.2006.01.033.

Fournier, R.O., 1999, Hydrothermal processes related to movement of fluid from plastic into brittle rock in the magmatic-epithermal environment: Economic Geology and the Bulletin of the Society of Economic Geologists, v. 94, p. 1193–1212., doi:10.2113/gsecongeo.94.8.1193.

Garzon, T., 2011, Discovery of the Colosa gold-rich porphyry deposit, *in* Proceedings, NewGenGold 2011 Conference, Perth, Western Australia: Louthean Media, Perth, p. 229–240.

Gustafson, L.B., and Hunt, J.P., 1975, The porphyry copper deposit at El Salvador, Chile: Economic Geology and the Bulletin of the Society of Economic Geologists, v. 70, p. 857–912, doi:10.2113/gsecongeo.70.5.857.

Hanes, R., Bakos, F., Fuchs, P., Žitňan, P., and Konečný, V., 2010, Exploration results of Au porphyry mineralizations in the Javorie stratovolcano: Mineralia Slovaca, v. 42, p. 15–33.

Harangi, Sz., Downes, H., Thirlwall, N., and Gméling, K., 2007, Geochemistry, petrogenesis and geodynamic relationships of Miocene calc-alkaline volcanic rocks in the Western Carpathian arc, Eastern Central Europe: Journal of Petrology, v. 48, p. 2261–2287, doi:10.1093/petrology/egm059.

Harris, C.R., Pettke, T., Heinrich, C.A., Rosu, E., Woodland, S., and Fry, B., 2013, Tethyan mantle metasomatism creates subduction geochemical signatures in non-arc Cu-Au-Te mineralizing magmas, Apuseni Mountains (Romania): Earth and Planetary Science Letters, v. 366, p. 122–136, doi:10.1016/j.epsl.2013.01.035.

Hedenquist, J.W., Arribas, A., and Reynolds Jr., T.J., 1998, Evolution of an intrusion-centred hydrothermal system: Far Southeast-Lepanto porphyry and epithermal Cu-Au deposits, Philippines: Economic Geology and the Bulletin of the Society of Economic Geologists, v. 93, p. 373–404, doi:10.2113/gsecongeo.93.4.373.

Heinrich, C.A., Driesner, T., Stefánsson, A., and Seward, T.M., 2004, Magmatic vapor contraction and the transport of gold from the porphyry environment to epithermal ore deposits: Geology, v. 32, p. 761–764, doi:10.1130/G20629.1.

Herrington, R., and Wilkinson, J., 1993, Colloidal gold and silica in mesothermal vein systems: Geology, v. 21, p. 539–542, doi:10.1130/0091-7613(1993)021<0539:CGASIM>2.3.CO;2.

Holtz, F., Johannes, W., Tamic, N., and Behrens, H., 2001, Maximum and minimum water contents of granitic melts: A reexamination and implications: Lithos, v. 56, p. 1–14.

Holtz, F., Sato, H., Lewis, J., Behrens, H., and Nakada, S., 2005, Experimental petrology of the 1991–1995 Unzen Dacite, Japan. Part I: Phase relations, phase composition and pre-eruptive conditions: Journal of Petrology, v. 46, p. 319–337, doi:10.1093/petrology/egh077.

Hurtig, N.C, and Williams-Jones, A.E., 2014, An experimental study of the transport of gold through hydration of AuCl in aqueous vapour and vapour-like fluids: Geochimica et Cosmochimica Acta, v. 127, p. 305-325, doi:10.1016/j.gca.2013.11.029.

Koděra, P., Lexa, J., Biroň, A., and Žitňan, J., 2010, Gold mineralization and associated alteration zones of the Biely Vrch Au-porphyry deposit, Slovakia: Mineralia Slovaca, v. 42, p. 33–56.

Koděra, P., Lexa, J., and Konečný, P., 2013: Application of CL-imaging and mineral geothermometry on the porphyry gold deposit Biely Vrch, Slovakia, *in* Proceedings of 12th SGA Biennial Meeting: Uppsala, Sweden, p. 817–820.

Konečný, V., Bezák, V., Halouzka, R., Konečný, P., Mihaliková, A., Marcin, D., Iglárová, Ľ., Panáček, A., Štohl, J., Žáková, E., Galko, I., Rojkovičová, Ľ., and Onačila, D., 1998, Explanation to the geological map of Javorie 1: 50 000: Geological Survey of Slovak Republic, Bratislava, 304 p.

Landtwing, M.R., Furrer, C., Redmond, P.B., Pettke, T., Guillong and M., Heinrich, C.A., 2010. The Bingham Canyon Porphyry Cu-Mo-Au Deposit. III. Zoned copper-gold ore deposition by magmatic vapor expansion: Economic Geology and the Bulletin of the Society of Economic Geologists, v.105, p. 91–118. doi:10.2113/gsecongeo.105.1.91

Loucks, R., 2012, Chemical characteristics, geodynamic settings, and petrogenesis of gold-ore-forming arc magmas: Centre of Exploration Targeting, University of Western Australia, Perth: Quarterly News, v. 20, p. 1–12.

Muntean, J.L., and Einaudi, M.T., 2000, Porphyry gold deposits of the Refugio district, Maricunga belt, northern Chile: Economic Geology and the Bulletin of the Society of Economic Geologists, v. 95, p. 1445–1472.

Muntean, J.L., and Einaudi, M.T., 2001, Porphyry-epithermal transition: Maricunga belt, northern Chile: Economic Geology and the Bulletin of the Society of Economic Geologists, v. 96, p. 743–772, doi:10.2113/gsecongeo.96.4.743.

Richards, J.P., 2009, Postsubduction porphyry Cu–Au and epithermal Au deposits: Products of remelting of subduction-modified lithosphere: Geology, v. 37, p. 247–250, doi:10.1130/G25451A.1.

Robelin, C., Chartrand, P., and Pelton, A.D., 2004, Thermodynamic evaluation and optimization of the ($NaCl+KCl+MgCl_2+CaCl_2+MnCl_2+FeCl_2+CoCl_2+NiCl_2$) system: The Journal of Chemical Thermodynamics, v. 36, p. 809–828, doi:10.1016/j.jct.2004.05.005.

Ruff, R.K., Stefanini, B., and Halga, S., 2012, Geology and petrography of the gold-rich Ciresata porphyry deposit, Metaliferi Mountains, Romania: Romanian Journal of Mineral Deposits, v. 85, p. 19–24.

Rutherford, M. J. and Hill, P. M., 1993, Magma ascent rates from amphibole breakdown: An experimental study applied to the 1980–-1986 Mount St. Helens eruption: Journal of Geophysical Research, v. 98, p. 19667–19686. doi:10.1029/93JB01613

Sillitoe, R.H., 2000, Gold-rich porphyry deposits: Descriptive and genetic models and their role in exploration and discovery: Reviews in Economic Geology, v. 13, p. 315–345.

Sillitoe, R.H., 2010, Porphyry copper systems: Economic Geology and the Bulletin of the Society of Economic Geologists, v. 105, p. 3–41, doi:10.2113/gsecongeo.105.1.3.

Ulrich, T., Günther, D., and Heinrich, C.A., 1999, Gold concentrations of magmatic brines and the metal budget of porphyry copper deposits: Nature, v. 399, p. 676–679, doi:10.1038/21406.

Vila, T., and Sillitoe, R.H., 1991, Gold-rich porphyry systems in the Maricunga belt, northern Chile: Economic Geology and the Bulletin of the Society of Economic Geologists, v. 86, p. 1238–1260, doi:10.2113/gsecongeo.86.6.1238.

Vila, T., Sillitoe, R.H., Betzhold, J., and Viteri, E., 1991, The porphyry gold deposit at Marte, northern Chile: Economic Geology and the Bulletin of the Society of Economic Geologists, v. 86, p. 1271–1286, doi:10.2113/gsecongeo.86.6.1271.

Williams-Jones, A.E., and Heinrich, C.A., 2005, Vapor transport of metals and the formation of magmatic–hydrothermal ore deposits: Economic Geology and the Bulletin of the Society of Economic Geologists, v. 100, p. 1287–1312, doi:10.2113/gsecongeo.100.7.1287.

Weis, P., Driesner, T., Heinrich, C.A., 2012, Porphyry-copper ore shells form at stable pressure – temperature fronts within dynamic fluid plumes: Science, v. 338, p. 1613–1616. doi:10.1126/science.1225009

Zajacz, Z., Candela, P.A., Piccoli, P.M., and Sanchez-Valle, C., 2012a, The partitioning of sulfur and chlorine between andesite melts and magmatic volatiles and the exchange coefficients of major cations: Geochimica et Cosmochimica Acta, v. 89, p. 81–101, doi:10.1016/j.gca.2012.04.039.

Zajacz, Z., Candela, P.A., Piccoli, P.M., Wälle, M., and Sanchez-Valle, C., 2012b, Gold and copper in volatile saturated mafic to intermediate magmas: Solubilities, partitioning, and implications for ore deposit formation: Geochimica et Cosmochimica Acta, v. 91, p. 140–159, doi:10.1016/j.gca.2012.05.033.